

**Assessment of the importance of the pairing interaction in the continuum**

R. Id Betan

*Departamento de Química y Física, FCEIA (UNR)-Instituto de Física Rosario (CONICET), Avenida Pellegrini 250, 2000 Rosario, Argentina*

G. G. Dussel

*Departamento de Física, FCEyN-UBA, Ciudad Universitaria, Pabellón 1, 1428 Buenos Aires, Argentina*

R. J. Liotta

*KTH, Alba Nova University Center, SE-10691 Stockholm, Sweden*

(Received 24 April 2008; published 27 October 2008)

A pairing interaction fitted to be applied in nuclei with active particles moving close to the continuum threshold or even immersed in the continuum itself is introduced. It is found that the effects of the nonresonant continuum upon physically meaningful quantities is unimportant. We applied the theory to heavy tin isotopes and good agreement between theory and the very few available experimental data is found.

DOI: [10.1103/PhysRevC.78.044325](https://doi.org/10.1103/PhysRevC.78.044325)

PACS number(s): 21.30.Fe, 21.60.-n, 24.30.Gd, 27.60.+j

**I. INTRODUCTION**

The treatment of many-body systems including the continuum part of the spectrum was first carried out by means of the continuum shell model (CSM) long ago [1]. Since then the CSM has been applied successfully in a number of situations (e.g., to explain halo nuclei [2]) or recently to study a variety of phenomena associated with the continuum [3]. By using the basis provided by the CSM a BCS formulation was presented in Ref. [4] and was later extended to the complex energy plane [5,6]. The BCS application to processes where the continuum plays an important role is justified. This has been shown in Refs. [7,8], where calculated quantities associated with relevant physical states as provided by a Hartree-Fock-Bogoliubov theory with proper boundary conditions are well approximated by the corresponding quantities evaluated within the BCS approximation. We therefore will investigate in this paper the importance of the proper continuum to the correlations induced by the pairing interaction acting on systems lying close to the continuum threshold or even immersed in the continuum itself. To this end we will start by defining the single-particle representation to be used in our calculations. In a second step we will assess the importance of the pairing correlation provided by bound and resonance states as compared to the one corresponding to the nonresonant continuum.

Section II describes the representation, Sec. III shows how the pairing interaction acts in the continuum, and a summary and conclusions are provided in the last section.

**II. BOX SINGLE-PARTICLE REPRESENTATION**

One usually describes the continuum by means of a basis set of states consisting of scattering waves (normalized to the delta Dirac function) or by plane waves with box boundary conditions. The advantage of the scattering waves is that one can readily impose proper (outgoing) boundary conditions, but for this one has to pay the price of dealing with functions of diverging norm. Instead, the functions in the box are normalized inside the box, but then one has somehow to

deduce the results provided by this basis in the limit when the dimension of the box goes to infinity. We have found that to derive clearly and without ambiguities the matrix elements of the pairing interaction among continuum states, it is more convenient to use the box representation. We therefore assume that the normal single-particle states are the eigenvectors of a Woods-Saxon potential, which are obtained by diagonalizing the potential in the box representation [9,10].

Within this representation one can obtain the bound states provided by the Woods-Saxon potential and the corresponding resonances as induced by the centrifugal barrier (and since we will deal only with neutrons there will be no Coulomb barrier). As we will show in the following, the resonances thus obtained are narrow. Wide resonances cannot be distinguished by the diagonalization method irrespective of the representation used. But all the resonances (i.e., the narrow as well as the wide ones) are the complex solutions of the Schrödinger equation with outgoing boundary conditions (Gamow states). The width of the resonance can be considered to be minus twice the imaginary part of the Gamow energy. But it is important to notice that this width corresponds to particle decay. If the system survives long enough in a given state then one can apply stationary formalisms, as we are doing here with the Gamow states. In this case all imaginary parts are small and the corresponding probabilities, such as those we will evaluate in the following, can be considered real numbers. Otherwise the stationary approximation is not valid and the probabilities become complex with large imaginary parts. One can say that these imaginary parts are the result of treating a time-dependent process within a time-independent formalism. The box representation fails to reveal wide resonances (see the following).

There is still another point that needs clarification. The particle decay width provided by the imaginary part of the Gamow energy is determined by the pure single-particle state moving on the continuum part of the spectrum. Even if the corresponding resonance is narrow, the single-particle state can be mixed with other configurations of more complicated character (such as, e.g., two-particle, one-hole states), inducing a wide

but meaningful resonance. That is, the single-particle state is fragmented into many pieces, inducing a wide resonance [11]. This is what usually happens in real nuclei. What one then measures is the particle-decay width of the fragments, as done, for example, in Ref. [12]. A similar feature is encountered in giant resonances, which are usually wide but whose observed widths are mostly a result of the spreading of the collective particle-hole resonance in many fragments. This spreading width is of the order of a few MeV, which is to be compared to the decay width of the order of a few tens of keV. The decay width can also be evaluated by using a RPA formalism in a basis consisting of Gamow states. One thus finds that the imaginary parts of the probabilities corresponding to the giant resonances are small whereas the imaginary parts of the resonance energies agree well with the measured particle decay width [13]. Wide resonances may also be important as doorway states in compound systems provided that the distance between neighboring resonances is large enough, as discussed, for example, in Ref. [14]. However, here we are dealing with single-particle resonances that have to live long enough to be observed (i.e., they have to be narrow). Therefore we consider that only narrow resonances are meaningful in this work.

The outgoing solutions of the Schrödinger equation are also the poles of the corresponding  $S$  matrix in the complex energy plane. Therefore we will call “poles” the set of bound and resonant states.

We will classify the states evaluated through the box representation in two groups. In one group will be all the nonresonant continuum states, which we will label with the letter  $c$ ; in the other will be all the bound and narrow resonant states (i.e., the poles), which we will label with the letter  $p$ . As a mean field we will choose a central plus spin-orbit Woods-Saxon potential determined by the parameters  $V_0 = 43.5$  MeV,  $V_{so} = 13.5$  MeV,  $r_0 = 1.27$  fm, and  $a = 0.7$  fm.

The bound single-particle states provided by the diagonalization of this potential for different values of  $R$  are presented in Table I. The corresponding experimental data, taken from Ref. [15], are also given (and differ very little from the ones given in Ref. [16]). One sees in this table that the calculated energies agree reasonably well with experiment as the radius of the box increases.

To make our presentation as clear as possible we will show with some detail the behavior of the resonances evaluated within the box representation, although perhaps many of these features are known [9,17].

In the continuum part of the spectrum (i.e., in the positive energy region), the number of states below a certain energy (cutoff energy) increases with the dimension of the box since the box boundary condition implies that the energies corresponding to a given partial wave are inversely proportional to  $R$  [18]. As a result, one also finds that as  $R$  increases the energy of the levels decreases. However, if the partial wave carries an angular momentum large enough a narrow resonance may appear. This would manifest itself such that the corresponding level will remain at a rather constant energy (plateau condition). This energy is the position of the narrow resonance. We present these features in Fig. 1, where the levels provided by the box corresponding to the partial wave

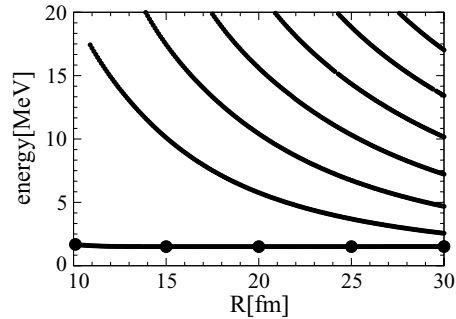


FIG. 1. Energy evolution of the box levels corresponding to the partial wave  $i_{13/2}$  as a function of the box radius  $R$  for the potential given in the text. The dots correspond to the resonance (see also Table II).

$i_{13/2}$  are given for a cutoff energy of 20 MeV. One sees that the level energies decrease (and the number of levels increases) as  $R$  increases. However, at about 1.5 MeV the first level remains at a rather constant energy throughout the interval of  $R$  values presented in the figure. This is a resonance. Since resonances appear as a result of the trapping of the system by the centrifugal barrier, one expects that the corresponding single-particle wave function  $R_{nlj}(r)$  should be localized within a region extending to a radius  $d$  defined by the barrier. We will thus define the localization  $L$  of a given state as the probability of finding the system in that state within the distance  $d$ , that is,

$$L_{nlj} = \int_0^d R_{nlj}^2(r) r^2 dr. \quad (1)$$

As was already mentioned, the Gamow energies are complex quantities and their imaginary parts can be interpreted as minus twice the width of the resonances. Therefore for narrow resonances the imaginary parts of the energies are, in absolute value, small, but also the imaginary parts of the localization are small for narrow resonances.

The  $L$  values with  $d = 10$  fm are shown in Table II for the low lying poles in  $^{132}\text{Sn}$ . The Gamow states as well as the corresponding states evaluated by using the box representation are given. One thus sees that for the state  $i_{13/2}$  the Gamow energy has a very small (in absolute value) imaginary part and that the localization is practically unity (real). That is, this is a narrow resonance, as expected by consideration of the large centrifugal barrier associated with it. The corresponding values of  $L$  provided by the box are larger than 99% for all box dimensions, showing that narrow resonances are indeed localized.

One sees in Fig. 2 that the evolution of the box states corresponding to the resonance  $j_{15/2}$  depends on the box radius. As one chooses larger values of  $R$  starting from  $R = 10$  fm, the energy of the first level, which for small values of  $R$  represents the resonance, will eventually diminish but the resonance will still manifest itself since then the second level will remain constant at the resonance energy. At even larger box dimensions the energy of the second level will also diminish and the third level will become the resonance. This trend goes on for larger and larger  $R$  values since at the

TABLE I. Bound single-particle states corresponding to neutrons outside  $^{132}\text{Sn}$ . The energies are in MeV and the box radius  $R$  is in fm. The experimental data are from Ref. [15].

State	Exp.	$R = 10$	$R = 15$	$R = 20$	$R = 25$	$R = 30$
$2f_{7/2}$	-2.450	-2.516	-2.471	-2.527	-2.504	-2.462
$3p_{3/2}$	-1.596	-1.396	-1.389	-1.381	-1.405	-1.367
$1h_{9/2}$	-0.889	-0.965	-0.954	-0.922	-1.018	-0.919
$3p_{1/2}$	-0.794	-0.690	-0.731	-0.759	-0.737	-0.754
$2f_{5/2}$	-0.445	-0.377	-0.262	-0.232	-0.193	-0.193

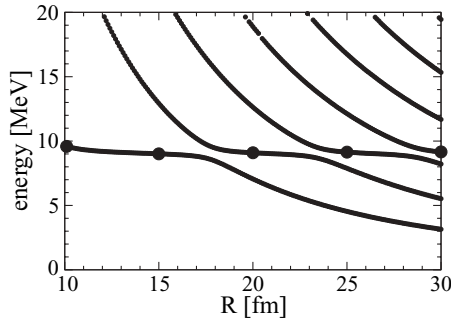


FIG. 2. Energy evolution of the box levels corresponding to the partial wave  $j_{15/2}$  as a function of the box dimension. The dots correspond to the box resonances shown in Table II.

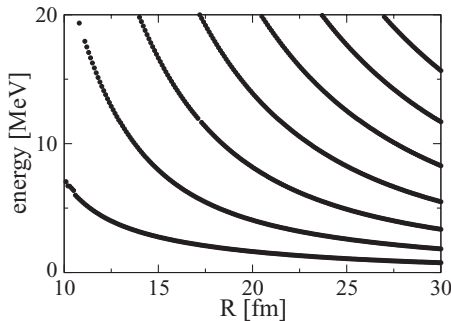


FIG. 3. Energy evolution of the box levels corresponding to the partial wave  $d_{5/2}$  as a function of the box dimension.

limit of  $R = \infty$  the number of levels is also infinite. One thus sees that up to about  $R = 17$  fm the resonance corresponds to the first (lowest) box state. From  $R = 17$  fm to  $R = 24$  fm it is the second state that is the resonance, from  $R = 24$  fm to  $R = 29$  fm it is the third state, and at  $R = 30$  fm the resonance becomes the fourth state. That the dots in Fig. 2 correspond indeed to the resonance changing state as the box size increases can be verified by looking at the localization. Thus, we evaluated  $L$  at  $R = 20$  fm for the first box state  $j_{15/2}$  and found that its value is much smaller than the one corresponding to the second state that according to Table II is  $L = 0.905$ . The same occurs at other box dimensions; that is, the localization corresponding to the resonance is always much larger than the one corresponding to the nonresonant states. However, this localization is approximately unity only for very narrow resonances, indicating that narrow resonances may be considered as quasibound states. An example of a pole that cannot be considered a narrow resonance is shown in Fig. 3, where no plateau is seen for the very wide state  $d_{5/2}$ , and all the box states have a very small localization.

One sees in Table II that for the very narrow resonance  $i_{13/2}$  the localization is  $L = 0.991$ , and for the resonance  $i_{11/2}$ , which is 380 keV wide,  $L = 0.751$ . It thus becomes clear that the reason for these different values of the localization is that the box state representing the resonance corresponds to the position of the resonance, which otherwise is distributed throughout its width. In the box representation used here the way to include the width is by decreasing the distance between the box levels (i.e., by increasing the dimension of the box). Using this procedure one verifies that there is a convergence in the evaluated quantities when reaching a certain value of  $R$ ,

TABLE II. Resonant neutron states in  $^{132}\text{Sn}$  evaluated through the box diagonalization as a function of the box radius  $R$ . The complex energies in the second column were evaluated by using the computer code GAMOW [19]. Energies are given in MeV and the box radius is in fm. The box state number (labeled by *State*) as well as the localization  $L$  [Eq. (1)] are also given.

State	Gamow states		$R = 10$			$R = 15$			$R = 20$			$R = 30$		
	Energy	$L$	Energy	State	$L$	Energy	State	$L$	Energy	State	$L$	Energy	State	$L$
$d_{5/2}$	$1.249 - i2.030$	$(-0.099, -1.841)$	—	—	—	—	—	—	—	—	—	—	—	—
$i_{13/2}$	$1.452 - i0.00002$	$(0.992, 0.000)$	1.652	1	1.	1.508	1	0.993	1.506	1	0.992	1.518	1	0.991
$g_{9/2}$	$3.470 - i0.443$	$(0.893, -0.286)$	5.423	2	1.	3.645	2	0.806	4.475	3	0.517	3.931	4	0.524
$g_{7/2}$	$5.500 - i1.818$	$(1.285, -0.679)$	—	—	—	—	—	—	—	—	—	—	—	—
$i_{11/2}$	$7.780 - i0.190$	$(1.005, -0.065)$	8.306	1	1.	7.688	1	0.897	7.818	2	0.905	7.981	3	0.751
$j_{15/2}$	$9.019 - i0.126$	$(0.981, -0.051)$	9.611	1	1.	9.010	1	0.928	9.090	2	0.923	9.159	4	0.834

which in box calculations is usually not larger than  $R = 30$  fm in medium and heavy nuclei. This is a procedure that we will follow in the present paper.

We evaluated all poles expected in this nuclear region, not only the states just discussed, by using the computer code GAMOW [19]. We show in Table II the complex energies and localizations thus calculated together with the corresponding values provided by the box diagonalization for different box radii. One sees in this table that the narrower a resonance is, the closest to unity is the localization. However, wide resonances have localizations that are complex with large imaginary parts, which, therefore, cannot be interpreted as probabilities.

The state  $1i_{13/2}$  is, according to its complex energy, a very narrow resonance that lies at an energy of 1.452 MeV, which is close to the value provided by the diagonalization for a box radius larger than 15 fm. The Gamow state  $1j_{15/2}$  is wider and therefore the evolution of the state seen in Fig. 2 shows that the plateau changes from one level to the next one as  $R$  increases. However, the energy of the different plateaus thus formed remains constant at about 9 MeV, in good agreement with the real part of the corresponding Gamow energy.

It is interesting to analyze whether the wave function of a narrow Gamow state is similar to the one corresponding to the wave function provided by the diagonalization procedure in the box. For this we will analyze the level  $i_{13/2}$  of Fig. 1 that we have assumed to represent the resonance. In Fig. 4 we compare the Gamow wave function (real as well as imaginary parts) with the wave functions provided by the box representation for  $R = 15$  fm and  $R = 30$  fm. As expected for this very narrow resonance, the imaginary part of the Gamow wave function is negligibly small for distances at least up to 30 fm. The agreement between the corresponding real part and the box wave functions is excellent, confirming our previous conclusions.

The important point in this analysis is that the narrow resonance wave functions are localized within the nucleus. Therefore the matrix elements of the pairing interaction acting upon resonance states with given values of angular momenta should have values similar to the ones corresponding to bound

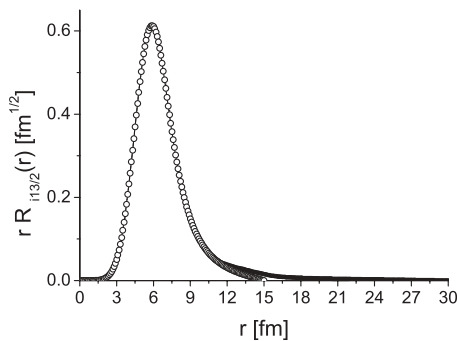


FIG. 4. Comparison between the Gamow wave function for the state  $1i_{13/2}$  and the corresponding resonant state obtained by the box diagonalization for  $R = 15$  fm and  $R = 30$  fm. The imaginary part of the Gamow wave function is negligible, while the real part coincides, within the precision of the figure, with the case  $R = 30$  fm. Even the case  $R = 15$  fm [for which  $R_{13/2}(r = 15 \text{ fm}) = 0$ ] is very similar to the other two cases, except at the tail.

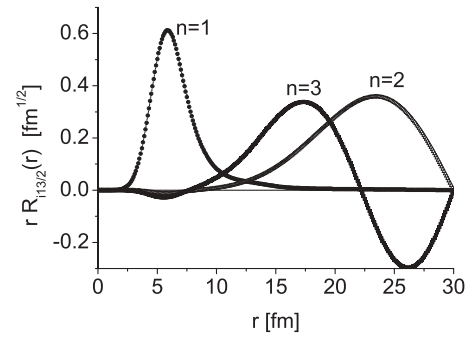


FIG. 5. Wave functions for the first three box states (labeled by  $n$ ) corresponding to the partial wave  $i_{13/2}$  evaluated at  $R = 30$  fm.

states. Instead, continuum states are not localized and the continuum wave functions are distributed along the whole space inside the box. As an example we show in Fig. 5 the wave function corresponding to the three first states in Fig. 1 at  $R = 30$  fm. The first of these is the resonance already shown in Fig. 4; the other two are states in the nonresonant continuum. One thus sees that the continuum states are indeed distributed throughout the box.

There is still one uncertainty regarding the resonances, namely that their localization depends on the width of the resonance. The question is at which value of the imaginary part of the energy the pole loses its physical relevance to become a part of the continuum background. To answer this question we first consider the  $3d_{5/2}$  Gamow state in Table II at (1.249,  $-2.030$ ) MeV. We present the corresponding wave function in Fig. 6. One sees that it spreads outside the nucleus and that its imaginary part is large. It is also seen in the evolution of the levels as a function of the dimension of the box corresponding to the partial wave  $d_{5/2}$  (see Fig 3), which shows no plateau. So this state belongs to the nonresonant continuum.

As an example of another state that does not show any plateau, we present in Fig. 7 the partial wave  $g_{7/2}$ . In this case the energy of the pole is, according to Table II, (5.500,  $-1.818$ ) MeV. However, the pole  $2g_{9/2}$ , at an energy of (3.470  $- i0.443$ ) MeV, can be recognized by using the box diagonalization. This can be seen in Fig. 8, where the evolution of the levels corresponding to the partial wave  $g_{9/2}$  is presented. Although here the plateau is rather weak, it can still be seen at

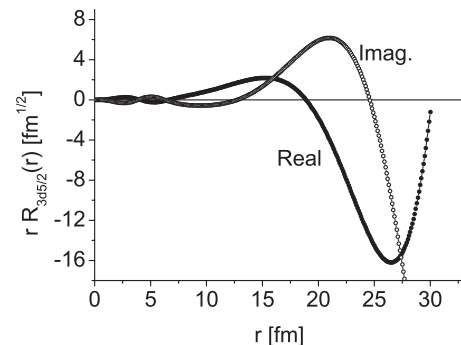


FIG. 6. Real and imaginary parts of the complex Gamow wave function corresponding to the state  $3d_{5/2}$  at (1.249,  $-2.030$ ) MeV.

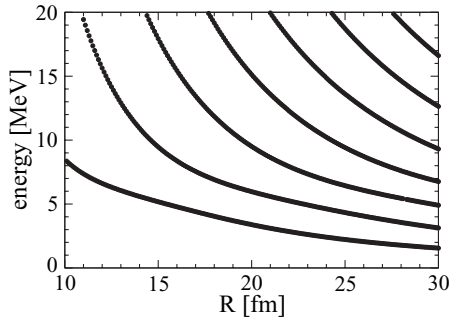


FIG. 7. Evolution of the levels corresponding to the partial wave  $g_{7/2}$  as a function of the box dimension.

about 3 MeV. Owing to the width of the resonance the energy differs rather much from the one corresponding to the pole (cf. Table II).

It is important to notice that it is the box representation that provides the energies that can be compared with experiment.

As a result of this discussion one can assert that very narrow resonances (of the order of a few keV or less) show a behavior very similar to that of bound states. That is, the resonance survives such a long time that the state can be considered quasistationary. But when the width of a resonance reaches a few hundred keV, it becomes increasingly difficult to identify any plateau in the evolution of the corresponding box levels. In other words, it is the presence of a plateau that determines whether the resonance will be considered as a pole in this formulation.

### III. THE PAIRING INTERACTION

In this section we will define the pairing interaction in the continuum following the procedure that has been shown to be very successful in bound systems [20]. We start with the two-particle wave function  $\Phi_{n_1 n_2}^{JM}$ , where  $n_i$  labels all the quantum numbers corresponding to particle  $i$ . By taking for the pairing force the monopole component of the contact delta interaction [i.e.,  $V(\mathbf{r}_1, \mathbf{r}_2) = -V_0 \delta(\mathbf{r}_2 - \mathbf{r}_1)$ ], the matrix elements take the form

$$\langle \Phi_{n_1 n_2}^{JM} | V_P | \Phi_{n_3 n_4}^{JM} \rangle = (-)^{l_1+l_3} \delta_{J0} \delta_{n_1 n_2} \delta_{n_3 n_4} \langle \Phi_{n_1 n_1}^{00} | V | \Phi_{n_3 n_3}^{00} \rangle$$

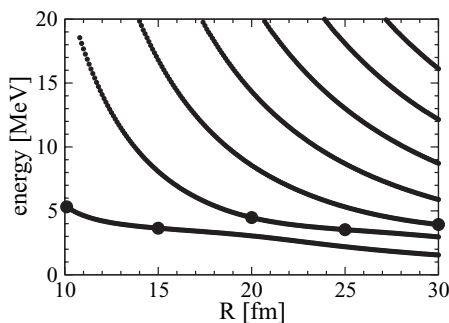


FIG. 8. Evolution of the partial wave  $g_{9/2}$  as a function of the box dimension. The dots correspond to the box resonances shown in Table II

where, with standard notation [21],

$$\langle \Phi_{n_1 n_1}^{00} | V | \Phi_{n_3 n_3}^{00} \rangle = -(-)^{l_1+l_3} \frac{V_0}{2} \hat{j}_1 \hat{j}_3 I_{n_1 n_3}$$

and

$$I_{n_1 n_3} = \frac{1}{4\pi} \int_0^\infty R_{n_1}^2(r) R_{n_3}^2(r) r^2 dr. \quad (2)$$

The state  $n_1$  (and  $n_3$ ) can be a pole or a continuum state. In what follows we will call “poles” only bound states and physically meaningful resonances (i.e., states that correspond to some plateau in the box representation). Therefore there are three types of integrals, namely  $I^{pp}$ ,  $I^{pc}$ , and  $I^{cc}$ .

The integrals in Eq. (2) are dependent on the states. It is customary to replace them by their average value to have a constant pairing interaction [20]. The average is defined as

$$I_{av} = \frac{\sum_{m,n} (2j_n + 1)(2j_m + 1) I_{n,m}}{\sum_{m,n} (2j_n + 1)(2j_m + 1)}. \quad (3)$$

The evaluation of these averages will allow us to estimate the dependence of the integrals in Eq. (2) on the nuclear volume  $V_N$  and on the box volume  $V$ .

As we have seen, the radial wave functions  $R_n$  have a very different behavior for the case of pole states as compared to nonresonant states. Because to this we will consider separately the pole-pole, pole-continuum, and continuum-continuum cases.

#### A. Pole-pole case $I^{pp}$

Table III displays the average value of the integrals for the pole states ( $I_{av}^{pp}$ ) obtained for different box sizes. The striking feature is the remarkable independence of  $I_{av}^{pp}$  on the box size. This is a manifestation of the localization of the poles and, therefore, one can use the standard values of the pairing strength for this case (i.e.,  $G_p \approx g/A$ ) [22].

It is possible to arrive at the same conclusion by using general arguments. Since the pole wave function is localized, most of it is inside the nuclear volume  $V_N = \frac{4\pi}{3} R_N^3$ . This important property makes it possible to approximate  $R_n(r)$  by the function  $R_n^{\text{loc}}(r)$  defined as

$$R_n^{\text{loc}}(r) = \begin{cases} \frac{R_n(r)}{\sqrt{\int_0^{R_N} R_n^2(x) x^2 dx}} & (r \leq R_N) \\ R_n^{\text{loc}}(r) = 0 & (r > R_N). \end{cases} \quad (4)$$

TABLE III. Average value of the integrals involving pole states for different box volumes  $V$ .

$R$ (fm)	$V$ (fm <sup>3</sup> )	$I_{av}^{pp} \times 10^{-3}$ (fm <sup>-3</sup> )
15	14,137	0.358
20	33,510	0.351
25	65,450	0.340
30	113,097	0.321
Average relative deviation		3.5%

The integral becomes

$$I_{n_1 n_2}^{\text{pp}} = \frac{1}{4\pi} \int_0^{R_N} [R_{n_1}^{\text{loc}}(r)]^2 [R_{n_2}^{\text{loc}}(r)]^2 r^2 dr. \quad (5)$$

Since  $R_n(r)$  are real functions the integrands  $I(r)$  in Eqs. (4) and (5) are positive functions and a value of  $r = \rho$  exists ( $0 \leq \rho \leq R_N$ ) such that

$$\int_0^{R_N} I(r) r^2 dr = I(\rho) R_N^3 / 3 = I(\rho) \frac{3V_N}{4\pi}. \quad (6)$$

Equation (5) can then be written as

$$I_{n_1 n_2}^{\text{pp}} = I_{n_1 n_2, \text{av}} / V_N, \quad (7)$$

where

$$I_{n_1 n_2, \text{av}} = \frac{R_{n_1}^2(\rho_{12}) R_{n_2}^2(\rho_{12})}{3R_{n_1}^2(\rho_1) R_{n_2}^2(\rho_2)}. \quad (8)$$

That is, the pairing strength  $G_p$  corresponding to the pole-pole sector will be multiplied by a constant  $I_{\text{av}}$ , which will be the average of the values  $I_{n_1 n_2, \text{av}}$ .

### B. Continuum-continuum case $I^{\text{cc}}$

Table IV displays the average value of the integrals for the continuum states obtained for different box sizes. We also display the average value of the volume times the integral ( $V \times I_{\text{av}}^{\text{cc}}$ ). The striking feature here is that  $V \times I_{\text{av}}^{\text{cc}}$  does not depend on the box size, and therefore one can use for the pairing interaction a strength, which is proportional to  $1/V$ .

Again, it is possible to understand this result on general arguments. To do so we will treat the nonresonant continuum by using Cartesian coordinates, as one does in the description of homogeneous superconductor materials [23]. In this case the box state is defined by the linear momentum  $\mathbf{k} = (k_x, k_y, k_z)$ . The normalized single-particle wave function is, therefore,

$$R(\mathbf{k}, \mathbf{r}) = e^{i\mathbf{k} \cdot \mathbf{r}} / \sqrt{V}, \quad (9)$$

where  $V = L^3$  and  $L$  is the length of the cubic box.

Notice that, as the pairing interaction is extracted from the delta force and the wave function does not contain information related to the relative motion part of the two particles in time reversal states, one can replace  $e^{ik(r_1 - r_2)}$  by unity [23]. Therefore,

$$I^{\text{cc}} = \frac{1}{V^2} \int_0^V dx dy dz = \frac{1}{V}. \quad (10)$$

TABLE IV. Average value of the integrals involving continuum states for different box volumes  $V$ .

$R$ (fm)	$V$ (fm <sup>3</sup> )	$I_{\text{av}}^{\text{cc}} \times 10^{-4}$ (fm <sup>-3</sup> )	$V \times I_{\text{av}}^{\text{cc}}$
15	14,137	0.878	1.24
20	33,510	0.346	1.16
25	65,450	0.171	1.12
30	113,097	0.097	1.10
Average relative deviation			3.9%

TABLE V. Average value of the integrals involving pole and continuum states for different box volumes  $V$ .

$R$ (fm)	$V$ (fm <sup>3</sup> )	$I_{\text{av}}^{\text{pc}} \times 10^{-4}$ (fm <sup>-3</sup> )	$V \times I_{\text{av}}^{\text{pc}}$
15	14,137	1.060	1.50
20	33,510	0.440	1.47
25	65,450	0.218	1.43
30	113,097	0.131	1.42
Average relative deviation			2.1%

### C. Pole-continuum case $I^{\text{pc}}$

Table V displays the average value of the integrals involving pole and continuum states obtained for different box sizes. We also display the average value of the integral times the volume. Again the independence of this quantity on the box size is remarkable, and therefore one can use for the pairing interaction a strength that goes as  $1/V$ .

By using the general arguments one obtains, as before,

$$I^{\text{pc}} = \frac{1}{V} \frac{\sum_n (2j_n + 1) \int_0^R R_n^2(r) r^2 dr}{\sum_n (2j_n + 1)} = \frac{1}{V}. \quad (11)$$

### D. The pairing Hamiltonian

We consider for convenience a pairing interaction with constant strength, but the results to be presented do not depend very much on this approximation, as expected. In Sec. III I we will avoid this approximation and the energy-dependent matrix elements will be properly evaluated.

As already shown within the constant pairing strength one finds that the pairing interaction largely depends on the volume as  $1/V_N \propto 1/A$  (see also Refs. [24,25]) for the pole states. This feature has been confirmed experimentally since the beginning of the application of pairing interactions in nuclei [22] and has been confirmed rather recently [24]. However, we have seen that the interaction goes as  $1/V$  for the part involving continuum states (see also Ref. [23]). The pairing Hamiltonian thus becomes

$$H_P = H_{\text{sp}} - G_p P_p^\dagger P_p - G_c P_p^\dagger P_c - G_c P_c^\dagger P_p - G_c P_c^\dagger P_c, \quad (12)$$

where

$$G_p = \frac{I_{\text{av}} V_0}{V_N}, \quad (13)$$

$$G_c = \frac{V_0}{V}, \quad (14)$$

$$P_p^\dagger = \sum_{nm>0} (-)^{j_n - m} a_{nm}^\dagger a_{n-m}^\dagger, \quad (15)$$

$$P_c^\dagger = \sum_{vm>0} (-)^{j_v - m} a_{vm}^\dagger a_{v-m}^\dagger, \quad (16)$$

where  $I_{\text{av}}$  is the average value introduced in Eq. (3).

The label  $p$  ( $c$ ) indicates pole (continuum) pairing states. The single-particle pole states are labeled by  $n$  and the nonresonant continuum states are labeled by  $v$ . Since  $G_c/G_p \propto V_N/V$  the strength of the pairing interaction acting upon states in

the continuum diminishes with respect to the corresponding pole strength as the volume of the box increases. One may therefore be tempted to conclude that the continuum contribution will be negligible as the dimension of the box goes to infinity. But before reaching such conclusion the physical quantities should be evaluated first and then the limit should be performed. This we intend to do in the following.

By making the usual quasiparticle transformation the pairing gaps for pole and continuum states become

$$\Delta_p = G_p \Delta_p \sum_n \frac{2j_n + 1}{4E_n} + G_c \Delta_c \sum_v \frac{2j_v + 1}{4E_v}, \quad (17)$$

$$\Delta_c = G_c \Delta_p \sum_n \frac{2j_n + 1}{4E_n} + G_c \Delta_c \sum_v \frac{2j_v + 1}{4E_v},$$

where the quasiparticle energies  $E_n$  and  $E_v$  are given by

$$E_n = \sqrt{(\varepsilon_n - \lambda)^2 + \Delta_p^2}, \quad (18)$$

$$E_v = \sqrt{(\varepsilon_v - \lambda)^2 + \Delta_c^2} \quad (19)$$

and  $\lambda$  is the Fermi level.

The number of particles and the occupation numbers are

$$N = \sum_n (2j_n + 1)v_n^2 + \sum_v (2j_v + 1)v_v^2, \quad (20)$$

$$v_n^2 = \frac{1}{2} \left( 1 - \frac{\varepsilon_n - \lambda}{\sqrt{(\varepsilon_n - \lambda)^2 + \Delta_p^2}} \right), \quad (21)$$

$$v_v^2 = \frac{1}{2} \left( 1 - \frac{\varepsilon_v - \lambda}{\sqrt{(\varepsilon_v - \lambda)^2 + \Delta_c^2}} \right). \quad (22)$$

This constitutes the nonlinear system of equations for the unknown parameters  $\Delta_p$ ,  $\Delta_c$ , and  $\lambda$ . One can recognize here a state-dependent BCS set of equations. There are two different pairing parameters, one for the pole states and another one for the nonresonant continuum. As we have discussed in the previous section the pairing strength parameter can be written as  $G_p = g/A$ , where  $g$  depends upon the nuclear region and also on the number of shells included in the representation [22]. One thus gets  $V_0 = G_p V_N / I_{av} = \frac{4\pi}{3} r_0^3 g / I_{av}$ , where  $r_0$  is the radius parameter, which we will take as the one in the Woods-Saxon central potential. The strength in the continuum is  $G_c = V_0 / V$ , where  $V$  is the volume of the box.

### E. Quasiparticle energies

We solved the BCS equations by using  $g = 21$  [6] and obtained the quasiparticle energies corresponding to the valence orbits shown in Fig. 9. One sees in this figure that the order of the levels change from one state to another as the shells are filled following the same pattern as the one expected in bound nuclei, thus showing that the pole states determine the behavior of the system in the continuum. The scarce available experimental data [16] agree well with our calculation, but it is not possible to give a definite answer to

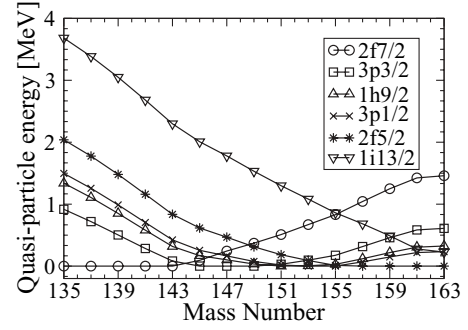


FIG. 9. Quasiparticle excitation energies as a function of the mass number in heavy Sn isotopes for an energy cutoff of 30 MeV and a box size of  $R = 30$  fm.

whether the formalism is indeed appropriate to describe the effect of pairing interactions in the continuum until more data become available.

The quasiparticle energies shown (for bound as well as for resonant states) were evaluated by using a box of radius  $R = 30$  fm and a cutoff energy of 30 MeV. We also performed the calculations using smaller cutoffs and have found that the results do not change appreciably even using the rather low value of 10 MeV.

To investigate the convergence of the pole quasiparticle energies as a function of the box size we show in Table VI those energies as well as the corresponding occupation probabilities for an energy cutoff of 30 MeV and for 16 valence states. One sees that the convergence is satisfactory even for wide resonances (cf. Table II).

### F. Gap parameters

A major aim of this paper is to investigate the importance of the nonresonant continuum in building up physically meaningful unstable states. This we can do by noticing that from Eqs. (17) one gets

$$V \Delta_c = V_0 \Delta_c \sum_n \frac{2j_n + 1}{4E_n} + V \Delta_p \left( 1 - \sum_n G_p \frac{2j_n + 1}{4E_n} \right), \quad (23)$$

where  $G_c = V_0 / V$  was used. If the nonresonant continuum is neglected then

$$1 - \sum_n G_p \frac{2j_n + 1}{4E_n} = 0$$

and, therefore, the product  $V \Delta_c$  would be independent of the box size. We show in Table VII this product for an energy cutoff of 30 MeV as a function of the number of particles. One indeed sees that  $V \Delta_c$  is virtually independent of the box size

TABLE VI. Quasiparticle energy and occupation probability as a function of the box size for the energy cutoff of 30 MeV and  $N = 16$ . The energies are in MeV and the box radius is in fm.

State	$R = 10$		$R = 15$		$R = 20$		$R = 25$		$R = 30$	
	$E$	$v^2$								
$2f_{7/2}$	2.075	0.793	1.875	0.831	1.914	0.838	1.867	0.836	1.878	0.837
$3p_{3/2}$	1.686	0.528	1.415	0.556	1.419	0.552	1.392	0.555	1.399	0.560
$1h_{9/2}$	1.716	0.402	1.434	0.403	1.445	0.392	1.403	0.417	1.417	0.401
$3p_{1/2}$	1.767	0.348	1.494	0.332	1.489	0.340	1.476	0.326	1.458	0.348
$2f_{5/2}$	1.920	0.259	1.709	0.216	1.731	0.211	1.742	0.196	1.715	0.207
$1i_{13/2}$	3.400	0.066	3.054	0.056	2.994	0.059	3.051	0.054	3.017	0.056
$2g_{9/2}$	6.933	0.015	5.076	0.020	4.505	0.025	4.980	0.020	5.313	0.017
$1i_{11/2}$	9.755	0.007	9.036	0.006	9.164	0.006	9.258	0.006	8.388	0.007
$1j_{15/2}$	11.042	0.006	10.327	0.005	10.405	0.005	10.456	0.004	10.426	0.004

for each isotope even when the volume of the box changes 27 times (i.e., from  $R = 10$  fm to  $R = 30$  fm). The last line in the table shows the relative deviation with respect to the mean value. It is less than 1% for the isotopes considered. We found the same behavior for other energy cutoffs.

Another feature that shows this is the evolution of the continuum gap  $\Delta_c$  as a function of the box size. In Figure 10 we plotted  $\Delta_c$  for different isotopes and box sizes using an energy cutoff of  $E = 30$  MeV. One can see that the continuum gap becomes negligible as the box radius increases.

In Figs. 11 and 12 one can see the convergence of the pairing gap parameter and the Fermi level, respectively, as a function of the box size for different isotopes (with an energy cutoff of 30 MeV). These features again confirm that the nonresonant continuum can be disregarded in describing unstable nuclei.

### G. Particle number

An additional probe of the importance of the nonresonant continuum can be performed by analyzing its contribution to the number of particles (20). To do this we first use the standard procedure to replace sums by integrals [23], that is,

$$\frac{1}{V} \sum_n f(k_n) \rightarrow \int g(\varepsilon) f(\varepsilon) d\varepsilon \quad \text{with} \quad g(\varepsilon) = \frac{3\sqrt{2m^3}}{\hbar^3 \pi^3} \sqrt{\varepsilon}. \tag{24}$$

TABLE VII. Continuum gap parameter times box volume as a function of the box size for an energy cutoff of 30 MeV and for a particle numbers from  $N = 2$  to  $N = 8$ . The values of  $\Delta_c \times V$  are given in unit of  $\text{fm}^3 \text{ MeV}$ .

$R$ (fm)	$V$ ( $\text{fm}^3$ )	$N = 2$	$N = 4$	$N = 6$	$N = 8$
10	4189	685	938	1119	1268
15	14,137	670	921	1102	1254
20	33,510	668	916	1096	1250
25	65,450	683	939	1124	1279
30	113,087	676	929	1111	1266
Relative deviation		0.89%	0.86%	0.81%	0.72%

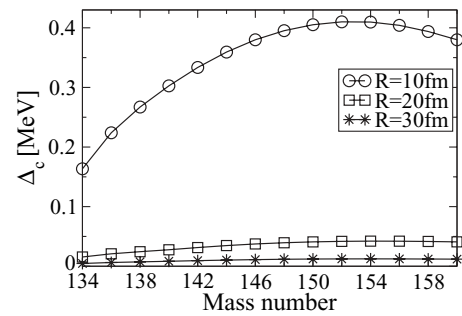


FIG. 10. Evolution of the continuum gap parameter for different isotopes as the box increases for the energy cutoff of 30 MeV.

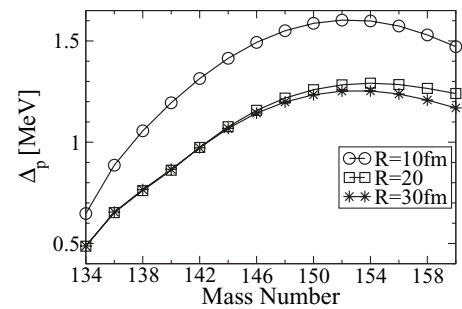


FIG. 11. Evolution of the gap parameter for different isotopes as the box increases for an energy cutoff of 30 MeV.

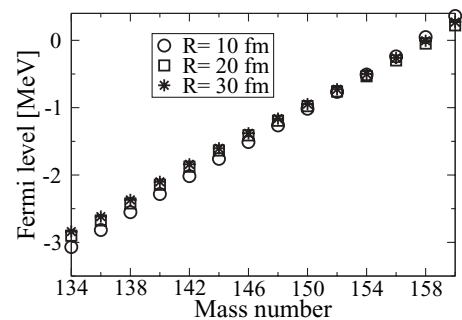


FIG. 12. Evolution of the Fermi level for different isotopes as the box increases for an energy cutoff of 30 MeV.

TABLE VIII. The product  $P = N_c V \sqrt{|\lambda|}$  (in units of  $\text{fm}^3 \text{MeV}^{1/2}$ ) as a function of the box size and the particle number  $N$  for an energy cutoff of 30 MeV. The Fermi level  $\lambda$  is give in MeV.

$R$ (fm)	$V$ ( $\text{fm}^3$ )	$N = 2$		$N = 4$		$N = 6$		$N = 8$	
		$P$	$-\lambda$	$P$	$-\lambda$	$P$	$-\lambda$	$P$	$-\lambda$
10	4189	31	3.161	58	2.906	82	2.640	104	2.369
15	14,137	34	3.098	65	2.854	92	2.600	120	2.340
20	33,510	38	3.133	71	2.886	151	2.625	133	2.358
25	65,450	54	3.118	104	2.875	102	2.620	199	2.359
30	113,087	48	3.078	92	2.828	134	2.572	176	2.309
Relative deviation	19.6%	20.5%		21.4%		22.5%			

Notice that the single-particle density contains only the nonresonant part. The particle number equation becomes

$$N = \sum_n v_n^2 + V \int g(\varepsilon) v^2(\varepsilon) d\varepsilon. \quad (25)$$

Since the first term in this equation does not depend on the box size for large enough values of  $R$ , the second term will not depend on  $R$  either. We start the analysis of this second term,  $N_c$ , by noticing that for  $\Delta_c/|\varepsilon - \lambda| \ll 1$  (i.e., small  $\Delta_c$ ) one can write

$$v^2(\varepsilon) = \frac{1}{2} \left( 1 - \frac{\varepsilon - \lambda}{\sqrt{(\varepsilon - \lambda)^2 + \Delta_c^2}} \right) \simeq \frac{\Delta_c^2}{4|\varepsilon - \lambda|^2} \quad (26)$$

and

$$N_c = V \int g(\varepsilon) v^2(\varepsilon) d\varepsilon \simeq \frac{V \Delta_c^2}{4} \int \frac{g(\varepsilon) d\varepsilon}{|\varepsilon - \lambda|^2}. \quad (27)$$

Since  $\Delta_c \propto 1/V$  (Sec. III F) one obtains, after performing the integral,  $N_c \propto \frac{1}{V \sqrt{|\lambda|}}$ , and therefore the product  $P = N_c V \sqrt{|\lambda|}$  should be independent on  $R$  if our assumption that  $\Delta_c$  is small is valid. We show this product in Table VIII for an energy cutoff of 30 MeV and for particle numbers from 2 to 8. One sees that for each value of the particle number the value of  $P$  is rather constant, with a dispersion of about 20%.

## H. Binding energies

So far we used  $g = 21$ , which we took from Ref. [6]. We want now to evaluate binding energies to compare with available experimental data. To do this we proceed as usual and write the BCS Hamiltonian as

$$H_{\text{BCS}} = B + \sum_{nm} E_n \alpha_{nm}^+ \alpha_{nm} + \sum_{vm} E_v \alpha_{vm}^+ \alpha_{vm}, \quad (28)$$

where the binding energy is

$$B = \sum_{nm} v_n^2 (\varepsilon_n - \lambda) + \sum_{vm} v_v^2 (\varepsilon_v - \lambda) + V_{\text{pair}} \quad (29)$$

and the pairing energy has the form

$$V_{\text{pair}} = -\frac{\Delta_p}{2} \sum_n (2j_n + 1) u_n v_n - \frac{\Delta_c}{2} \sum_v (2j_v + 1) u_v v_v. \quad (30)$$

It is worthwhile to point out that the BCS equations do not have any nontrivial solution for normal systems. In particular, in the nucleus  $^{48}\text{Ca}$  the BCS equations give zero gap whereas exact numerical solutions provide a couple of MeV of correlation energy [26]. This feature is still present when the continuum is included.

We evaluated the binding energies  $B$  using for the pairing strength the value  $g = 22.5$ , which fits the experimental binding energy of  $^{134}\text{Sn}$ . In Table IX we show the results of our calculations and the few available experimental data. Again, here, it is encouraging to see that, for the only measured isotope (i.e.,  $^{136}\text{Sn}$ ), the agreement between theory and experiment is excellent.

One may think that any calculation that includes the continuum in some reasonable way would provide binding energies that would be in equally good agreement with each other and with experiment or, in other words, that all reasonable calculations in heavy Sn isotopes would provide similar results. To show that this is not the case we notice that in a recent shell-model calculation adjusted to treat neutron-rich nuclei [28] it was found that  $B = 18.56$  MeV in  $^{138}\text{Sn}$ , well outside the corresponding value shown in Table IX.

Finally, it is worthwhile noticing that even the experimental binding energies in these isotopes may disagree with each other substantially. Thus, in a recent paper [29] the binding energy of  $^{134}\text{Sn}$  was reported to be  $B = 5.906$  MeV (cf. the corresponding value in Table IX). We re-evaluated our Sn isotopes by adjusting the pairing strength to obtain that experimental energy, which we did with  $g = 18.4$ . This gives for  $^{136}\text{Sn}$  the value  $B = 11.426$  MeV (i.e., a deviation of 910 KeV with respect to the nowadays accepted value). It

TABLE IX. Binding energies  $B$  for heavy Sn isotopes. The experimental results are from Ref. [27]. A box radius of  $R = 30$  fm and a cutoff energy of 30 MeV were used in the calculations.

Isotope	Experimental (MeV)	Calculated (MeV)
$^{134}\text{Sn}$	6.390	6.390
$^{136}\text{Sn}$	12.336	12.321
$^{138}\text{Sn}$	–	17.764
$^{140}\text{Sn}$	–	22.692

TABLE X. Single-particle states and corresponding energies (MeV) in the core  $^{132}\text{Sn}$  evaluated by using the delta interaction matrix elements [Eq. (2)] and the box representation. In the third column is the pairing gap (in MeV) and in the last column is the occupation probability  $v^2$  corresponding to the quasiparticle states in the nucleus  $^{148}\text{Sn}$  (i.e.,  $N = 16$ ) The states are ordered in three groups: bound states (with negative energies), resonances (as determined by the box procedure), and some selected continuum states.

State	Energy	Gap	$v^2$
<b>Bound</b>			
$2f_{7/2}$	-2.527	1.122	$8.7 \times 10^{-1}$
$3p_{3/2}$	-1.381	0.523	$6.2 \times 10^{-1}$
$1h_{9/2}$	-0.922	1.568	$4.0 \times 10^{-1}$
$3p_{1/2}$	-0.759	0.230	$4.4 \times 10^{-2}$
$2f_{5/2}$	-0.232	0.747	$9.2 \times 10^{-2}$
<b>Resonances</b>			
$i_{13/2}$	1.506	2.000	$1.0 \times 10^{-1}$
$g_{9/2}$	4.475	0.661	$3.3 \times 10^{-3}$
$i_{11/2}$	7.818	1.488	$6.6 \times 10^{-3}$
$j_{15/2}$	9.090	1.900	$8.3 \times 10^{-1}$
<b>Continuum</b>			
$s_{1/2}$	0.995	0.040	$8.3 \times 10^{-5}$
$d_{3/2}$	4.469	0.174	$2.3 \times 10^{-4}$
$f_{7/2}$	2.681	0.090	$1.3 \times 10^{-4}$

thus seems that experimental efforts to measure these binding energies are well motivated.

### I. Influence of the continuum background

We have shown that the contribution of the continuum background to the physical quantities diminish and eventually vanishes as the dimension of the box goes to infinity. We have performed our studies by using a constant pairing interaction. We now want to show that bound states and narrow resonances are also overwhelmingly more important than states in the continuum background even if the force is dependent upon the configurations in which the pairs of nucleons move. This calculation will also enable us to probe whether the use of the constant pairing interaction is justified. To do this we will include the matrix elements of the delta force [Eq. (2)] without performing any average of their values. We thus evaluated the gaps and occupation probabilities  $v^2$  corresponding to bound, resonant, and continuum configurations by using the box representation with a box radius of  $R = 20$  fm and a cutoff energy of 30 MeV. The corresponding results are shown in Table X, where even the single-particle energies are given. In the table the states have been collected in three groups.: the bound states, the resonances, and some selected continuum states. One notices that the gaps and occupation probabilities

in the first group are of the same order of magnitude as the corresponding quantities in the second group. Instead, the gaps in the third group are about one order of magnitude smaller as compared with those in the first two groups. Even more striking is the difference in the occupation probabilities, which are on average three orders of magnitude smaller than the previous ones. Considering that this difference would even be larger as the box dimension increases, one can conclude that continuum states do not influence the dynamics of unstable nuclei. This is just in agreement with the conclusions reached in the previous case of constant pairing strength.

Another important feature that one notices in this calculation is that the evaluated quantities agree well with the ones calculated previously. This can be seen by comparing the energies in Table X with the corresponding ones in Tables I and II, while the occupation probabilities can be compared with those given in Table VI. The average pairing gap in this energy-dependent case is 1.201 MeV, which agrees well with the corresponding value in Fig. 11. One thus confirms the validity of the constant pairing interaction in BCS calculations.

## IV. SUMMARY AND CONCLUSIONS

In this paper we have introduced a pairing interaction fitted to be applied in nuclei with active particles moving close to the continuum threshold or even immersed in the continuum itself. For this we took into consideration the property that resonant wave functions are localized within the nuclear volume whereas states in the continuum are distributed over the whole space. Using these properties we found that the pairing strength  $G_p$  corresponding to bound and resonant states is different than the pairing strength  $G_c$  acting upon continuum states. We found that the effects of the nonresonant continuum upon physically meaningful quantities are not important. We applied the theory to heavy Sn isotopes and found very good agreement between the calculated quantities and the few available experimental data. We argued that experimental efforts to measure binding energies in these nuclei would be most welcome to probe theories that are designed to treat the continuum part of the spectrum, including the theory presented here.

## ACKNOWLEDGMENTS

Fruitful suggestions by N. Sandulescu and discussions with T. Vertse are gratefully acknowledge. This work was supported in part by UBACYT X-053, Carrera del Investigador Científico, PIP-5287 (CONICET-Argentina), and PICT 21605 (ANPCT-Argentina).

[1] C. Mahaux and H. A. Weidenmüller, *Shell Model Approach to Nuclear Reactions* (North-Holland, Amsterdam, 1969).  
 [2] H. Esbensen, G. F. Bertsch, and K. Hencken, Phys. Rev. C **56**, 3054 (1997).

[3] A. Volya and V. Zelevinsky, Phys. Rev. C **74**, 064314 (2006).  
 [4] N. S. Sandulescu, R. J. Liotta, and R. Wyss, Phys. Lett. **B394**, 6 (1997).

- [5] R. Id Betan, N. Sandulescu, and T. Vertse, Nucl. Phys. **A771**, 93 (2006).
- [6] G. G. Dussel, R. Id Betan, R. J. Liotta, and T. Vertse, Nucl. Phys. **A789**, 182 (2007).
- [7] M. Grasso, N. Sandulescu, N. Van Giai, and R. J. Liotta, Phys. Rev. C **64**, 064321 (2001).
- [8] I. Hamamoto and B. R. Mottelson, Phys. Rev. C **68**, 034312 (2003).
- [9] C. H. Maier, L. S. Cederbaum, and W. Domcke, J. Phys. B **13**, L119 (1980).
- [10] L. Zhang, S. G. Zhou, J. Meng, and E. G. Zhao, Phys. Rev. C **77**, 14312 (2008).
- [11] S. Fortunato, A. Insolia, R. J. Liotta, and T. Vertse, Phys. Rev. C **54**, 3279 (1996).
- [12] S. Fortier, D. Beaumel, and S. Gals *et al.*, Phys. Rev. C **52**, 2401 (1995).
- [13] P. Curutchet, T. Vertse, and R. J. Liotta, Phys. Rev. C **39**, 1020 (1989).
- [14] N. Auerbach and V. Zelevinsky, Nucl. Phys. **A781**, 67 (2007).
- [15] P. Hoff *et al.*, Phys. Rev. Lett. **77**, 1020 (1996).
- [16] [www.nndc.bnl.gov](http://www.nndc.bnl.gov).
- [17] J. Dobaczewski, W. Nazarewicz, T. R. Werner, J. F. Berger, C. R. Chinn, and J. Decharge, Phys. Rev. C **53**, 2809 (1996).
- [18] P. Bonche, S. Levit, and D. Vautherin, Nucl. Phys. **A427**, 278 (1984).
- [19] T. Vertse, K. F. Pál, and Z. Balogh, Comput. Phys. Commun. **27**, 309 (1982).
- [20] A. M. Lane, *Nuclear Theory. Pairing Force Correlations and Collective Motion* (Benjamin, New York, 1964).
- [21] R. D. Lawson, *Theory of the Nuclear Shell Model* (Oxford University Press, Oxford, 1980).
- [22] S. L. Kissinger and R. A. Sorensen, Rev. Mod. Phys. **35**, 853 (1963).
- [23] A. L. Fetter and J. D. Walecka, *Quantum Theory of Many-Particle Systems* (McGraw-Hill, New York, 1971).
- [24] M. Dufour and A. P. Zuker, Phys. Rev. C **54**, 1641 (1996).
- [25] A. Bohr and B. R. Mottelson, *Nuclear Structure*, Vol. II (World Scientific, Singapore, 1998), p. 653.
- [26] A. Volya, B. A. Brown, and V. Zelevinsky, Phys. Lett. **B509**, 37 (2001).
- [27] [ie.lbl.gov/toi2003/MassSearch.asp](http://ie.lbl.gov/toi2003/MassSearch.asp).
- [28] S. Sarkar and M. Saha Sarkar, arXiv:0802.3740v1 [nucl-th].
- [29] M. Dworschak *et al.*, Phys. Rev. Lett. **100**, 072501 (2008).